Cosolvent Exclusion Drives Protein Stability in TMAO and Betaine Solutions.

Pritam Ganguly[†1], Dominik Bubák[2], Jakub Polák[2], Patrik Fagan[3], Martin Dračínský[4], Nico F. A. van der Vegt[5], Jan Heyda[2], and Joan-Emma Shea[*1,6]

[1]*Department of Chemistry and Biochemistry, University of California at Santa Barbara, Santa Barbara, California 93106, USA.*

[2]*Department of Physical Chemistry, University of Chemistry and Technology, Prague, Technická 5, 166 28 Prague 6, Czech Republic.*

[3]*Department of Analytical Chemistry, University of Chemistry and Technology, Prague, Technická 5, 166 28, Prague 6, Czech Republic.*

[4]*Institute of Organic Chemistry and Biochemistry, Czech Academy of Sciences, Flemingovo nám. 2, 160 00 Prague, Czech Republic.*

[5]*Eduard-Zintl-Institut für Anorganische und Physikalische Chemie, Technische Universität Darmstadt, Alarich-Weiss-Straße 10, Darmstadt 64287, Germany.*

[6]*Department of Physics, University of California at Santa Barbara, Santa Barbara, California 93106, USA.*

Abstract

Using a combination of molecular dynamics simulation, dialysis experiments, and electronic circular dichroism measurements, we studied the solvation thermodynamics of proteins in two osmolyte solutions, trimethylamine N-oxide (TMAO) and betaine. We showed that existing force fields are unable to capture the solvation properties of the proteins lysozyme and ribonuclease T1 and that the inaccurate parameterization of protein-osmolyte interactions in these force-fields promoted an unphysical strong thermal denaturation of the trpcage protein. We developed a novel force field for betaine (the KBB force field) which reproduces experimental solution Kirkwood-Buff integrals and density. We further introduced appropriate scaling to protein-osmolyte interactions in both the betaine and TMAO force-fields which led to successful reproduction of experimental protein-osmolyte preferential binding coefficients for lysozyme and ribonuclease T1 and prevention of the unphysical denaturation of trpcage in osmolyte solutions. Correct parameterization of protein-TMAO interactions also led to the stabilization of the collapsed conformations of a disordered elastin-like peptide, while the uncorrected parameters destabilized the collapsed structures. Our results establish that the thermodynamic stability of proteins in both betaine and TMAO solutions is governed by osmolyte exclusion from proteins.

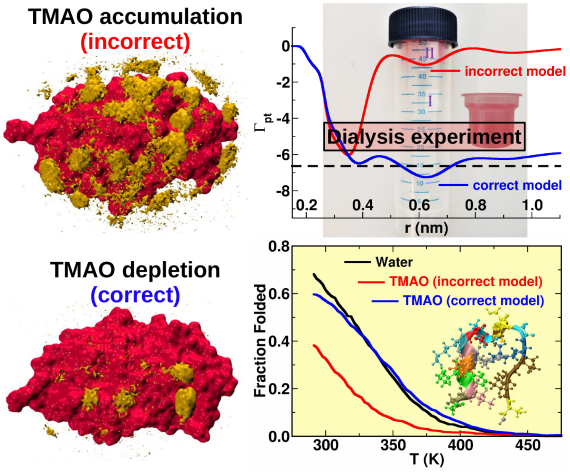

Osmolytes are small organic solutes that are essential for cell viability as they regulate the structure and function of cellular proteins under conditions of osmotic stress. The protein-protective characteristics of the amine-based or sugar-based osmolytes have generally been attributed to their unfavorable interaction with the peptide groups, leading to their exclusion from the protein surface.[1–7] However, the protein-protective mechanism for one particular osmolyte, trimethylamine N-oxide (TMAO), which counteracts urea-denaturation of cellular proteins in higher order marine mammals and cartilaginous fishes,[8,9] remains elusive and disputed.[6,10–16]

Earlier osmometry and densimetry/dialysis experiments suggested preferential exclusion of TMAO from peptide groups and folded proteins.[1,4,17] More recently, using MD simulations, Mondal and coworkers showed that the TMAO-protein preferential binding coefficient[18–21] could be positive or negative, depending on the amino acid composition of the protein.[22] However, the TMAO-peptide pref-

[†]E-mail: pganguly@chem.ucsb.edu
[*]E-mail: shea@chem.ucsb.edu

erential binding coefficients were higher for the folded conformations of the proteins than for the unfolded conformations. Thus, TMAO was found to promote the folded conformations of the proteins. Earlier, a similar mechanism was proposed for hydrophobic polymers in TMAO.[23,24] Subsequently, Liao et al. also proposed a similar mechanism for TMAO on an elastin-like polypeptide and contrasted that with betaine, which was found to promote collapsed peptide conformations through the classical osmolyte-exclusion mechanism from the peptide surface.[25] In contrast, recent experimental data indicated exclusion of TMAO from a short polyalanine chain.[26] In our earlier studies[27,28] and in a recent review,[29] we highlighted the importance of correctly capturing the TMAO solvation properties in MD simulations and their effects on predicting protein stability. In the current work, we address the importance of protein-TMAO interaction parameters in MD simulation. Here we perform new dialysis experiments to further understand protein solvation in TMAO solutions, benchmark our simulations against earlier and new experimental data, reparameterize protein-TMAO interactions and predict the thermodynamic mechanism for protein stability in TMAO. In addition, we compare our results with betaine to examine if the protein-protective mechanism for TMAO is indeed a special one among other osmolytes.

We are further interested in the comparison between TMAO and betaine because both are naturally occurring, zwitterionic, amine-based protein-protective osmolytes with a hydrophobic trimethylamine headgroup attached to a negatively charged polar group. For TMAO, there exist all-atom models which correctly capture solvation properties of binary TMAO-water systems.[29–31] Here, we first tested if the existing betaine force fields are capable of capturing betaine solvation properties in binary betaine-water solutions. We tested three betaine force fields: a) the CHARMM[32] force field adapted by Ma et al.,[33] b) a modification of the CHARMM force field by Ma et al. (the Ma force field),[33] c) a further modification of the Ma force field by Liao et al. (the Liao force field).[25] In Figure S1 in the Supporting Information, we plotted the betaine-betaine Kirkwood-Buff integral (KBI)[34,35] and the solution density for 1–3 molar betaine-water solutions. We found that none of the force fields could reproduce the experimental betaine-betaine KBI[36] and the density[37] simultaneously. Hence, we developed a new betaine force field (the details are in the Supporting Information) which reproduce both the solution density and the betaine-betaine KBI. We note that the development of KBI-based force field parameters, pioneered by Smith et al.,[38] has widely been applied in studying aqueous mixtures.[28,39–45] Along with solution density and KBIs of binary betaine-water systems, our newly developed betaine force field (the Kirkwood-Buff betaine, KBB) also reproduced the experimental triglycine-betaine preferential binding coefficient[7,33,46] (Figure S2 in the Supporting Information). No significant difference in the betaine-betaine KBI and in the triglycine-betaine preferential binding coefficient were observed when the TIP3P[47] and the SPC/E[48] water models were used with the KBB model for betaine. We used the KBB betaine model for simulating all our protein-betaine systems in this work, in conjunction with the TIP3P water model, to be consistent with the protein model used (AMBER99SB-ILDN[49]) in this work (see the Supporting Information for more details).

Thus far, there have been only a few MD simulation studies that have aimed at reproducing experimental solvation properties of proteins in TMAO or betaine solutions.[6,25,26,30,33,50] The Netz TMAO model predicted the *m*-values for glycine, asparagine, valine and tryptophan homopolypeptides reasonable well, including the anomaly of negative *m*-value for tryptophan.[30] The *m*-value for trpcage miniprotein in TMAO was reproduced reasonably well by the García TMAO model, when appropriate scaling to the protein-osmolyte interactions was applied.[6] Folberth et al. showed that the Hölzl[31] and the Kast[51] TMAO force fields captured the TMAO exclusion from polyalanine but the force fields overestimated its absolute value.[26] The Ma[33] and the Liao[25] betaine force fields, as well as the newly developed KBB model, reproduced the preferential binding coefficient between triglycine and betaine (see Figure S2 in the supporting Information for the results with the KBB model).

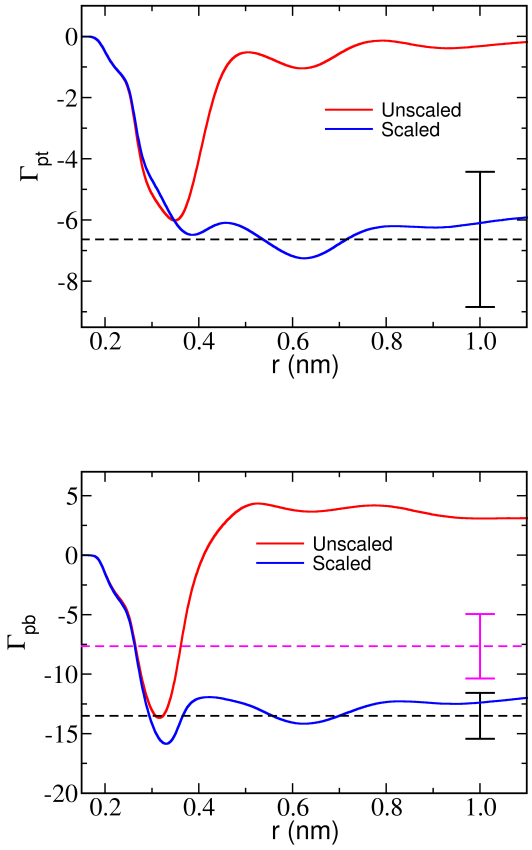

Figure 1: Upper panel: Shown are RNase T1-TMAO preferential binding coefficients (Γ_{pt}) for 1 M TMAO solutions. Lower panel: Lysozyme-betaine preferential binding coefficient (Γ_{pb}) for 2 M betaine solutions. Red curves: unscaled protein-osmolyte interactions, blue curves: protein-osmolyte van der Waals interactions scaled by 0.75. Black horizontal lines: results from dialysis experiments for TMAO[1] and betaine[52] by Timasheff et al. Magenta horizontal line: result from VPO measurements for betaine by Record et al.[53] The "per molal" value reported by Record et al. is multiplied by the molality of 2 M betaine solution (from simulation). The error bars indicate the errors in the experimental data. The experimental error for the TMAO system was calculated from the work by Record et al.[54]

However, for larger proteins, the availability of experimental preferential binding coefficient data for protein-TMAO or protein-betaine systems is very limited in the literature.[1,17,52–54] Nonetheless, we first examined if the TMAO or betaine force fields could reproduce experimental preferential binding coefficient data available in the literature. For that purpose, we chose lysozyme (for betaine)[52,53] and ribonuclease T1 (RNase T1) (for TMAO).[1] For lysozyme and RNase T1, we simulated the proteins in their native conformations using unbiased MD. In Figure 1, we plotted the preferential binding coefficient

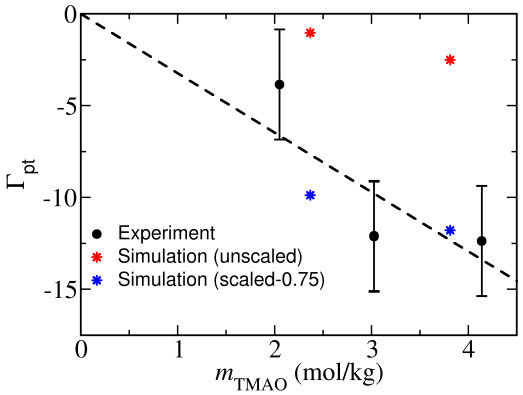

Figure 2: Lysozyme-TMAO preferential binding coefficient at different TMAO concentrations in molality. Black circles: new results from dialysis experiments. Black straight line: Linear regression of experimental data (y=-3.2x, R=0.79). Red stars: unscaled protein-TMAO interactions, blue stars: protein-TMAO van der Waals interactions scaled by 0.75.

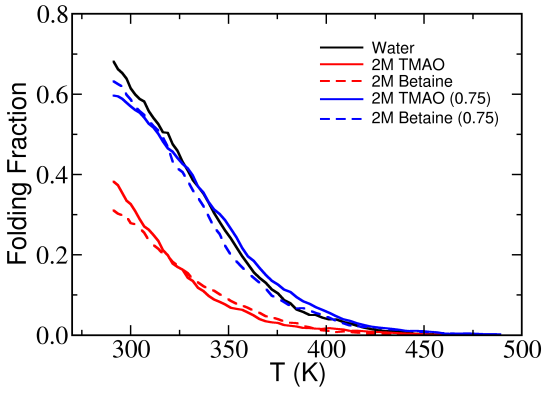

Figure 3: Folding fraction at different temperatures for trpcage in water, 2 M TMAO and 2 M betaine solutions. Red curves: unscaled protein-osmolyte interactions, blue curves: protein-osmolyte van der Waals interactions scaled by 0.75. The data for water are taken from our earlier work.[55]

between RNase T1 and TMAO (upper panel) for 1 M TMAO solution and between lysozyme and betaine (lower panel) for 2 M betaine solution. We found that the protein-osmolyte preferential binding coefficients had been significantly overestimated by our simulations (red solid lines) compared to experimental values (horizontal dashed lines). We used the Netz force field[30] for TMAO and the newly developed KBB for betaine for the data shown in Figure 1; however, as shown in Figures S3 (RNase T1-TMAO) and S4 (lysozyme-betaine) in the Supporting Information, different protein and osmolyte force field combinations yielded qualitatively similar results. In addition, we calculated lysozyme-TMAO preferential binding coefficient through dialysis experiments for 2, 3 and 4 molal TMAO solutions (experimental details are in the Supporting Information). Our new experimental data suggested strong depletion of TMAO from lysozyme surface (Figure 2). Assuming linearity between protein-cosolvent preferential binding coefficient and cosolvent molality,[46,53] we estimated the ratio between lysozyme-TMAO preferential binding coefficient and the TMAO molality to be ≈-3.2 per molal of TMAO. Similar to RNase T1, our simulation data could not capture the strong TMAO depletion from lysozyme (red stars in Figure 2).

Next, we examined if the TMAO force field was capable of capturing the osmolyte-induced protein-protection against thermal denaturation. For this purpose, we chose trpcage (NLYIQWLKDGGPSSGRPPPS), a native-folded alpha-helical miniprotein whose melting temperatures for different TMAO concentrations are known.[6] Using replica exchange molecular dynamics (REMD) simulations, we earlier predicted the melting temperature of trpcage to be very close to the experimental value in pure water.[55] Here, we performed REMD simulations of trpcage in 2 M TMAO solution. In Figure 3, we plotted the folding fraction of trpcage in pure water and in 2 M TMAO as a function of temperature. We found that the addition of 2 M TMAO to water significantly reduced the folding fraction and the melting temperature, corresponding to a 50% folding fraction. In contrast, experimental data predicted an increase in the melting temperature of trpcage in TMAO solutions (≈3 K increase at 2 M TMAO), indicating stabilization of the folded conformations explicitly.[6]

To understand the effects of betaine on the thermal stability of trpcage, we first performed electronic circular dichroism (ECD) experiments for trpcage in betaine solutions. Our experimental results predicted that betaine applies a mild destabilizing effect on trpcage, reducing its melting temperature by ≈3.5 K at 2 molal betaine concentration (Figure S5 in the Supporting Information). In contrast, our simulation with the KBB betaine model predicted very strong destabilization of the folded conformations by betaine (Figure 3). Our simulation predicted only ≈30% folded fraction for trpcage at 291.2 K, which was the lowest temperature considered for our REMD simulations. We note that a qualitatively similar observation was reported earlier with the CHARMM[32] betaine force field.[56] Our data strongly indicated the limitation in the protein-osmolyte force field combinations, despite the fact that the individual osmolyte force fields captured thermodynamic solution properties of the binary osmolyte-water systems and the protein force field predicted the correct melting behavior of folded proteins in pure water.[55] These observations also indicated that the efficient route to developing more accurate protein-osmolyte force field combinations may not be through the alteration of any of the osmolyte-osmolyte, osmolyte-water and the protein-water interactions, but rather through the correction of the direct protein-osmolyte interactions.

Hence, we scaled down protein-osmolyte van der Waals interactions to compensate for the over-accumulation of the osmolytes around the proteins. Figure 1 (blue curves) and Figure 2 (blue stars) show that if the protein-osmolyte van der Waals interactions are scaled by 75%, it significantly reduces protein-osmolyte preferential binding coefficients and predicts the data reasonably closer to the experimental data. Furthermore, Figure 1 shows that the effects of the force field correction are local. The preferential binding coefficient of the unscaled model steeply increases in the distance interval 0.4–0.5 nm where attractive van der Waals forces between TMAO and the protein surface occur. By contrast, this effect is significantly reduced for the scaled model. The scaled protein-osmolyte interaction parameters thus make corrections to the unphysical local accumulation of the osmolytes around the protein surfaces, as obtained by the uncorrected force field combinations. It should be noted that different experimental techniques, such as dialysis or vapor pressure osmometry, provide preferential binding coefficients for different thermodynamic conditions and the values may differ as seen in the lower panel of

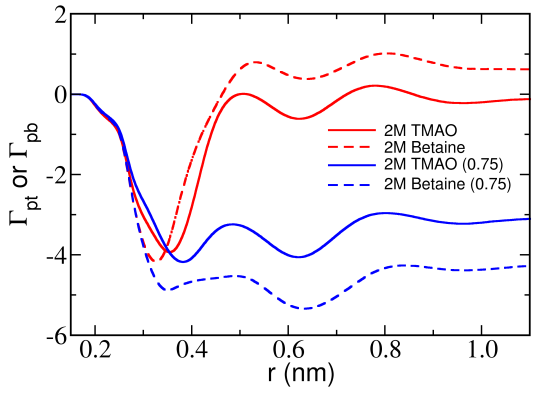

Figure 4: Trpcage-osmolyte preferential binding coefficient for 2 M TMAO and 2 M betaine solutions at 300 K. Red curves: unscaled protein-osmolyte interactions, blue curves: protein-osmolyte van der Waals interactions scaled by 0.75. The preferential binding coefficients for the folded and the unfolded states are separately shown in Figure S6 in the Supporting Information.

Figure 1. The thermodynamic conditions for the calculation of the preferential binding coefficients from our simulation also do not exactly match with the experimental conditions. A detailed discussion on this issue can be found in the work by Trout and coworkers[57] and in the Supporting Information.

Next, we applied the scaled protein-osmolyte interaction parameters to simulating the trpcage systems. We found that the unphysical strong destabilizing effects of the osmolytes could be corrected by the scaled protein-osmolyte interaction as it produced melting curves very similar to the ones obtained in pure water (see Figure 3). We note that in the experiments, 2 M TMAO was found to increase the melting temperature of trpcage only by ≈3 K with an error of ≈ ±2 K[6] and 2 molal betaine was found to decrease it by ≈3.5 K (see Table S7 in the Supporting Information). Next, we calculated the trpcage-osmolyte preferential binding coefficients using both unscaled and scaled protein-osmolyte interactions. The results at 300 K are shown in Figure 4. We found that the unscaled protein-osmolyte interaction yielded preferential accumulation of betaine around trpcage and predicted a near-zero preferential binding coefficient for TMAO. The scaled protein-osmolyte interaction resulted into preferential exclusion of both of the osmolytes. We note that in the work of García and coworkers, a scaled-down protein-TMAO van der Waals interaction also showed a higher preferential exclusion of TMAO from trpcage than the unscaled interaction and predicted more accurate *m*-value relative to experiments.[6] We next calculated the trpcage-osmolyte preferential binding coefficients separately for the folded and the unfolded conformations. We calculated the *m*-value for trpcage denaturation in TMAO to be −0.28 kJ/mol/M at 300 K, when the scaled protein-osmolyte interaction parameters are used. Our predicted *m*-value was close to the experimental value of −0.30 ± 0.15 kJ/mol/M (by Makhatadze and coworkers).[6] In contrast, with the unscaled protein-osmolyte interactions, we obtained an *m*-value of 0.47 kJ/mol/M, indicating unphysical strong destabilizing effects of TMAO. The trpcage-osmolyte preferential binding coefficients for the folded and unfolded conformations of trpcage are shown in Figure S6 in the Supporting Information. With an alternative approach, we calculated the trpcage *m*-value directly from the free-energies of unfolding where we used the fraction (f) of the folded conformations of trpcage to estimate the free-energy of unfolding as, $\Delta G = -RT\ \ln(\frac{1-f}{f})$. Thus, the *m*-value was obtained from the free-energies of unfolding in water ($\Delta G|_{c=0}$) and in the osmolyte solutions ($\Delta G|_{c=c}$) as, $\Delta G|_{c=c} = \Delta G|_{c=0} - mc$, with c being the osmolyte concentration (in molarity or molality scale). Using this approach, in Figure S7 in the Supporting Information, we compare the trpcage *m*-values at different temperatures, as obtained from our ECD experiments and the simulations. For both TMAO and betaine, we observed significant improvement in the simulated *m*-value with the scaled protein-osmolyte interactions, when compared with the experiments. Our results indicated that the scaled protein-osmolyte interaction provides a more accurate thermodynamic picture for the protein stability and we argue that both TMAO and betaine are preferentially excluded from trpcage.

In addition to the globular proteins, we studied the stabilization of a disordered elastin-like polypeptide (ELP) in TMAO-water solutions. For this purpose, we chose an ELP with VPGVG repeat units. Earlier experimental lower critical solution temperature (LCST) measurements showed that TMAO stabilizes the hydrophobic collapse of the $(\mathrm{VPGVG})_{120}$ peptide and significantly reduces its LCST.[25] Although a direct comparison with the experimental LCST measurements for such a large peptide was not possible with our all-atom REMD simulations, we studied the conformational stability of a smaller ELP, $(\mathrm{VPGVG})_4$, in pure water and in TMAO-water solutions. In Figure 5, we plot the distribution of the radius of gyration ($\mathrm{R_g}$) and the end-to-end distance (R_{ee}) of the ELP in pure water and in 2.1 M TMAO solutions. We found that the uncorrected protein-TMAO interactions (middle panel) did not stabilize the collapsed conformations of the ELP. In contrast, when the protein-TMAO van der Waals interactions were scaled by 75%, denoted by TMAO (0.75) in Figure 5, the probability for finding collapsed conformations of the peptide ($\mathrm{R_g} < 0.8$ nm) significantly increased. We note that the 75% scaling of the protein-TMAO interactions also reproduced the RNase T1-TMAO preferential binding coefficient for the protein/water/TMAO force field combination used in the studies of the ELP (Figure S3 in the Supporting Information). In Figure S8 in the Supporting Information, we further plot the radius of gyration (panel A), solvent-accessible surface area (SASA, panel B), and the number of residues with secondary structures or coil-like conformations (panel C) for the peptide at varying temperatures. We observed that the scaled protein-TMAO interactions led to peptide structures with reduced radius of gyration, reduced SASA, and enhanced secondary structures, while the uncorrected protein-TMAO interaction parameters led to swelling of the peptide, more significantly at the higher temperatures. We found that the TMAO-induced stabilization of the ELP correlated with the TMAO depletion from the peptide surface. Figure S8 (panel D) in the Supporting Information shows a significantly lower peptide-TMAO preferential binding coefficient at 301 K when the appropriate scaling to the peptide-TMAO interactions is applied. In Figure S9 in the Supporting Information, we show the corresponding most probable conformations of the ELP at 301 K, along with their respective probabilities and $\mathrm{R_g}$. The most probable ELP conformations further show that TMAO, if modeled correctly, increases the probability of finding compact peptide conformations with reduced $\mathrm{R_g}$.

In summary, we presented new dialysis experiments probing protein-osmolyte interactions, and used this new data, along with earlier experimental solvation data, to develop protein-osmolyte force-fields for TMAO and betaine solutions that correctly reproduce experimental solution KBIs and density for binary osmolyte-water systems, and protein-osmolyte preferential binding coefficients for ternary protein-osmolyte-water systems. Our osmolyte force fields

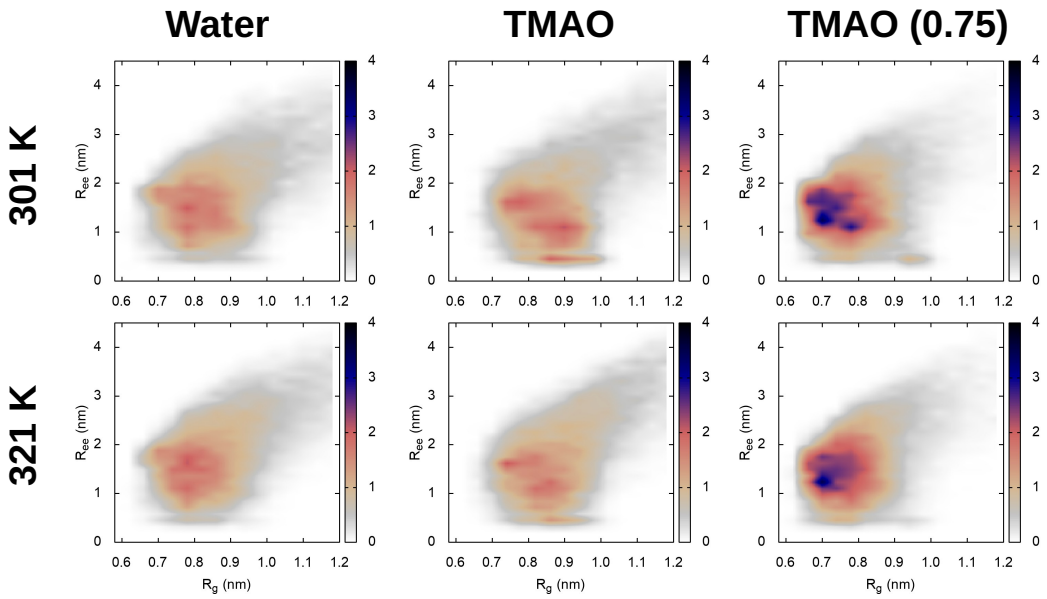

Figure 5: Distribution of the radius of gyration (R_g) and the end-to-end distance (R_{ee}) for $(VPGVG)_4$ in water and in 2.1 M TMAO solutions at 301 and 321 K temperatures. TMAO: unscaled protein-osmolyte interactions, TMAO (0.75): protein-TMAO van der Waals interactions scaled by 0.75.

are compatible with a range of protein force fields and water models. Importantly, we show that deficiencies in parameterization of earlier osmolyte force fields led to an inaccurate description of protein-osmolyte preferential binding coefficients, even when the force fields are capable of capturing correct thermodynamic properties for individual binary protein-water and osmolyte-water systems. Our work addresses the shortcomings of the MD parameters used in earlier studies and we show that protein-TMAO (and protein-betaine as well) preferential binding coefficients are overestimated if the protein-osmolyte interactions are not modeled correctly. In particular, we show that an excess protein-osmolyte interaction resulted into strong denaturation of trpcage, which contradicts experiments. Scaling-down the protein-osmolyte van der Waals interaction parameters compensates for the excess osmolyte-accumulation around proteins and corrects for the unphysical depression of trpcage melting temperature upon the addition of osmolytes. Artifacts associated with earlier incorrect parameterization of osmolyte force fields predicted that TMAO may act as an osmoprotectant without being excluded from proteins, and these results have popularized the idea that TMAO is a "special" osmolyte, fundamentally different than other protective osmolytes such as betaine, for example. Our simulations, consistent with the experimental thermodynamic stability of proteins in the osmolytes TMAO and betaine, however correctly predict preferential exclusion for both the osmolytes from protein surfaces. This is a critical point, as it shows that both osmolytes studied stabilize proteins through classical exclusion mechanism. In this respect, TMAO's action on proteins, in terms of osmolyte-depletion/accumulation, is not fundamentally different than that of betaine, with the same overarching mechanism explaining the action of both osmolytes.

ACKNOWLEDGMENTS

Simulations were performed on the Stampede 2 and the Frontera supercomputers at the Texas Advanced Computing Center at the University of Texas at Austin via the Extreme Science and Engineering Discovery Environment (XSEDE) grant (National Science Foundation (NSF) grant number TG-MCA05S027) and the Frontera grants (MCB21002 and MCB20034). The support from the National Science Foundation (NSF grant MCB-1716956) and the National Institutes of Health (NIH grant R01-GM118560-01A) is acknowledged. The Center for Scientific Computing at the California Nanosystems Institute (NSF Grant CNS-1725797) is also acknowledged. JH thanks the Czech Science Foundation (grant 20-24155S) for support. JP and DB acknowledges the financial support from a specific university research (A1_FCHI_2022_002). MD thanks the Czech Science Foundation (grant 22-15374S) for support.

SUPPORTING INFORMATION AVAILABLE

Simulation details, experimental details, equations for preferential binding coefficients using different experimental/simulation techniques, betaine-betaine KBIs and density for betaine-water solutions, betaine-triglycine preferential binding coefficients using KBB, protein-osmolyte preferential binding coefficients for different force field combinations, trpcage-osmolyte preferential binding coefficients for folded and unfolded conformations, ECD results for trpcage-stability in osmolyte solutions, trpcage *m*-values from ECD experiments and simulations, structural and thermodynamical properties of ELP in water and TMAO solutions (PDF).

Topology files for the KBB betaine model (ZIP).

REFERENCES

(1) Lin, T. Y.; Timasheff, S. N. Why Do Some Organisms Use a Urea-methylamine Mixture as Osmolyte? Thermodynamic Compensation of Urea and Trimethylamine N-oxide Interactions with Protein. *Biochemistry* **1994**, *33*, 12695–12701.

(2) Wang, A.; Bolen, D. W. A Naturally Occurring Protective System in Urea-Rich Cells: Mechanism of Osmolyte Protection

of Proteins against Urea Denaturation. *Biochemistry* **1997**, *36*, 9101–9108.

(3) Mukaiyama, A.; Koga, Y.; Takano, K.; Kanaya, S. Osmolyte Effect on the Stability and Folding of a Hyperthermophilic Protein. *Proteins Struct. Funct. Bioinfo.* **2008**, *71*, 110–118.

(4) Auton, M.; Bolen, D. W.; Rösgen, J. Structural Thermodynamics of Protein Preferential Solvation: Osmolyte Solvation of Proteins, Aminoacids, and Peptides. *Proteins* **2008**, *73*, 802–813.

(5) Cho, S. S.; Reddy, G.; Straub, J. E.; Thirumalai, D. Entropic Stabilization of Proteins by TMAO. *J. Phys. Chem. B* **2011**, *115*, 13401–13407.

(6) Canchi, D. R.; Jayasimha, P.; Rau, D. C.; Makhatadze, G. I.; García, A. E. Molecular Mechanism for the Preferential Exclusion of TMAO from Protein Surfaces. *J. Phys. Chem. B* **2012**, *116*, 12095–12104.

(7) Guinn, E. J.; Pegram, L. M.; Capp, M. W.; Pollock, M. N.; Record, M. T. Quantifying Why Urea is a Protein Denaturant, Whereas Glycine Betaine is a Protein Stabilizer. *Proc. Natl. Acad. Sci. U. S. A.* **2011**, *108*, 16932–16937.

(8) Yancey, P. H.; Somero, G. N. Counteraction of Urea Destabilization of Protein Structure by Methylamine Osmoregulatory Compounds of Elasmobranch Fishes. *Biochem. J.* **1979**, *183*, 317–323.

(9) Yancey, P. H.; Clark, M. E.; Hand, S. C.; Bowlus, R. D.; Somero, G. N. Living with Water Stress: Evolution of Osmolyte Systems. *Science* **1982**, *217*, 1214–1222.

(10) Ohto, T.; Hunger, J.; Ellen Backus, E.; Mizukami, W.; Bonn, M.; Nagata, Y. Trimethylamin-N-oxide: Hydration Structure, Surface Activity, and Biological Function Viewed by Vibrational Spectroscopies and Molecular Dynamics Simulations. *Phys. Chem. Chem. Phys.* **2017**, *19*, 6909–6920.

(11) Graziano, G. A rationale for the contrasting activity (towards globular proteins) of tert-butyl alcohol and trimethylamine N-oxide. *Phys. Chem. Chem. Phys.* **2012**, *14*, 13088–13094.

(12) Smolin, N.; Voloshin, V.; Anikeenko, A.; Geiger, A.; Winter, R.; Medvedev, N. N. TMAO and Urea in the Hydration Shell of the Protein SNase. *Phys. Chem. Chem. Phys.* **2017**, *19*, 6345–6357.

(13) Su, Z.; Mahmoudinobar, F.; Dias, C. L. Effects of Trimethylamine-N-oxide on the Conformation of Peptides and its Implications for Proteins. *Phys. Rev. Lett.* **2017**, *119*, 108102.

(14) Borgohain, G.; Paul, S. Model Dependency of TMAO's Counteracting Effect Against Action of Urea: Kast Model versus Osmotic Model of TMAO. *J. Phys. Chem. B* **2016**, *120*, 2352–2361.

(15) Kokubo, H.; Hu, C. Y.; Pettitt, B. M. Peptide Conformational Preferences in Osmolyte Solutions: Transfer Free Energies of Decaalanine. *J. Am. Chem. Soc.* **2011**, *133*, 1849–1858.

(16) Gao, M.; Held, C.; Patra, S.; Arns, L.; Sadowski, G.; Winter, R. Crowders and Cosolvents–Major Contributors to the Cellular Milieu and Efficient Means to Counteract Environmental Stresses. *ChemPhysChem* **2017**, *18*, 2951–2972.

(17) Hong, J.; Xiong, S. TMAO-Protein Preferential Interaction Profile Determines TMAO's Conditional In Vivo Compatibility. *Biophys. J.* **2016**, *111*, 1866–1875.

(18) Casassa, E. F.; Eisenberg, H. Thermodynamic Analysis of Multi-component Solutions. *Adv. Protein Chem.* **1964**, *19*, 287–395.

(19) Kuntz, I. D.; Kauzmann, W. Hydration of Proteins and Polypeptides. *Adv. Protein Chem.* **1974**, *29*, 239–345.

(20) Timasheff, S. N. The Control of Protein Stability and Association by Weak Interactions with Water: How Do Solvents Affect These Processes? *Annu. Rev. Biophys. Biomol. Struct.* **1993**, *22*, 67–97.

(21) Schellman, J. A. The Thermodynamic Stability of Proteins. *Annu. Rev. Biophys. Biophys. Chem.* **1987**, *16*, 115–137.

(22) Mukherjee, M.; Mondal, J. Unifying the Contrasting Mechanisms of Protein-Stabilizing Osmolytes. *J. Phys. Chem. B* **2020**, *124*, 6565–6574.

(23) Mondal, J.; Stirnemann, G.; Berne, B. J. When Does Trimethylamine N-Oxide Fold a Polymer Chain and Urea Unfold It? *J. Phys. Chem. B* **2013**, *117*, 8723–8732.

(24) Mondal, J.; Halverson, D.; Li, I. T. S.; Stirnemann, G.; Walker, G. C.; Berne, B. J. How Osmolytes Influence Hydrophobic Polymer Conformations: A Unified View from Experiment and Theory. *Proc. Natl. Sci. Acad. U. S. A.* **2015**, *112*, 9270–9275.

(25) Liao, Y.-T.; Manson, A. C.; DeLyser, M. R.; Noid, W. G.; Cremer, P. S. Trimethylamine N-oxide Stabilizes Proteins via a Distinct Mechanism Compared with Betaine and Glycine. *Proc. Natl. Acad. Sci. U.S.A.* **2017**, *114*, 2479–2484.

(26) Folberth, A.; Polák, J.; Heyda, J.; van der Vegt, N. F. A. Piezolyte-Structural Analysis of the Effects of Pressure and TMAO on the Peptide Solvation Shell. *J. Phys. Chem. B* **2020**, *124*, 6508–6519.

(27) Ganguly, P.; van der Vegt, N. F. A.; Shea, J.-E. Hydrophobic Association in Mixed Urea–TMAO Solutions. *J. Phys. Chem. Lett.* **2016**, *7*, 3052–3059.

(28) Ganguly, P.; Boserman, P.; van der Vegt, N. F. A.; Shea, J.-E. TMAO Counteracts Urea Denaturation by Inhibiting Protein-Urea Preferential Interaction. *J. Am. Chem. Soc.* **2018**, *140*, 483–492.

(29) Ganguly, P.; Polák, J.; van der Vegt, N. F. A.; Heyda, J.; Shea, J.-E. Protein Stability in TMAO and Mixed Urea–TMAO Solutions. *J. Phys. Chem. B* **2020**, *124*, 6181–6197.

(30) Schneck, E.; Horinek, D.; Netz, R. R. Insight into the Molecular Mechanisms of Protein Stabilizing Osmolytes from Global Force-field Variations. *J. Phys. Chem. B* **2013**, *117*, 8310–8321.

(31) Hölzl, C.; Kibies, P.; Imoto, S.; Frach, R.; Suladze, S.; Winter, R.; Marx, D.; Horinek, D.; Kast, S. M. Design Principles for High–pressure Force Fields: Aqueous TMAO Solutions from Ambient to Kilobar Pressures. *J. Chem. Phys.* **2016**, *144*, 144104.

(32) MacKerell, A. D.; Bashford, D.; Bellott, M.; Dunbrack, R. L.; Evanseck, J. D.; Field, M. J.; Fischer, S.; Gao, J.; Guo, H.; Ha, S.; Joseph-McCarthy, D.; Kuchnir, L.; Kuczera, K.; Lau, F. T. K.; Mattos, C.; Michnick, S.; Ngo, T.; Nguyen, D. T.; Prodhom, B.; Reiher, W. E.; Roux, B.; Schlenkrich, M.; Smith, J. C.; Stote, R.; Straub, J.; Watanabe, M.; Wiorkiewicz-Kuczera, J.; Yin, D.; Karplus, M. All-atom Empirical Potential for Molecular Modeling and Dynamics Studies of Proteins. *J. Phys. Chem. B* **1998**, *102*, 3586–3616.

(33) Ma, L.; Pegram, L. M.; Record, M. T.; Cui, Q. Preferential Interactions between Small Solutes and the Protein Backbone: A Computational Analysis. *Biochemistry* **2010**, *49*, 1954–1962.

(34) Kirkwood, J. G.; Buff, F. P. The Statistical Mechanical Theory of Solutions. I. *J. Chem. Phys.* **1951**, *19*, 774.

(35) Ben-Naim, A. *Molecular Theory of Solutions*; Oxford University Press: New York, 2006.

(36) Rösgen, J.; Pettitt, B. M.; Bolen, D. W.; An Analysis of

the Molecular Origin of Osmolyte-dependent Protein Stability. *Protein Sci.* **2007**, *16*, 733–743.

(37) Pitkänen, I.; Suuronen, J.; Nurmi, J. Partial Molar Volume, Ionization, Viscosity and Structure of Glycine Betaine in Aqueous Solutions. *J. Solution Chem.* **2010**, *39*, 1609–1626.

(38) Weerasinghe, S.; Smith, P. E. A Kirkwood-Buff Derived Force Field for Mixtures of Urea and Water. *J. Phys. Chem. B* **2003**, *107*, 3891–3898.

(39) Weerasinghe, S.; Smith, P. E. A Kirkwood-Buff Derived Force Field for Sodium Chloride in Water. *J. Chem. Phys.* **2003**, *119*, 11342.

(40) Weerasinghe, S.; Smith, P. E. A Kirkwood-Buff Derived Force Field for Methanol and Aqueous Methanol Solutions. *J. Phys. Chem. B* **2005**, *109*, 15080–15086.

(41) Klasczyk, B.; Knecht, V. Kirkwood–Buff Derived Force Field for Alkali Chlorides in Simple Point Charge Water. *J. Chem. Phys* **2010**, *132*, 024109.

(42) Lee, M. E.; van der Vegt, N. F. A. A New Force Field for Atomistic Simulations of Aqueous Tertiary Butanol Solutions. *J. Chem. Phys.* **2005**, *122*, 114509.

(43) Ganguly, P.; van der Vegt, N. F. A. Representability and Transferability of Kirkwood–Buff Iterative Boltzmann Inversion Models for Multicomponent Aqueous Systems. *J. Chem. Theory Comput.* **2013**, *9*, 5247–5256.

(44) Fyta M.; Netz, R. R. Ionic Force Field Optimization Based on Single-ion and Ion-pair Solvation Properties: Going Beyond Standard Mixing Rules. *J. Chem. Phys.* **2012**, *136*, 124103.

(45) Ploetz, E. A.; Karunaweera, S.; Bentenitis, N.; Chen, F.; Dai, S.; Gee, M. B.; Jiao, Y.; Kang, M.; Kariyawasam, N. L.; Naleem, N.; Weerasinghe, S.; Smith, P. E. A Kirkwood-Buff Derived Force Field for Peptides and Proteins: Philosophy and Development of KBFF20. *J. Chem. Theory Comput.* **2021**, *17*, 2964–2990.

(46) Capp, M. W.; Pegram, L. M.; Saecker, R. M.; Kratz, M.; Riccardi, D.; Wendorff, T.; Cannon, J. G.; Record, M. T. Interactions of the Osmolyte Glycine Betaine with Molecular Surfaces in Water: Thermodynamics, Structural Interpretation, and Prediction of m-Values. *Biochemistry* **2009**, *48*, 10372–10379.

(47) Jorgensen, W. L.; Chandrasekhar, J.; Madura, J. D.; Impey, R. W.; Klein, M. L. Comparison of Simple Potential Functions for Simulating Liquid Water. *J. Chem. Phys.* **1983**, *79*, 926.

(48) Berendsen, H. J. C.; Grigera, J. R.; Straatsma, T. P. The Missing Term in Effective Pair Potentials. *J. Phys. Chem.* **1987**, *91*, 6269–6271.

(49) Lindorff-Larsen, K.; Piana, S.; Palmo, K.; Maragakis, P.; Klepeis, J. L.; Dror, R. O.; Shaw, D. E. Improved Side-Chain Torsion Potentials for the Amber FF99sb Protein Force Field. *Proteins: Struct., Funct., Genet.* **2010**, *78*, 1950–1958.

(50) Adamczak, B.; Wieczór, M.; Kogut, M.; Stangret, J.; Czub, J. Molecular Basis of the Osmolyte Effect on Protein Stability: a Lesson from the Mechanical Unfolding of Lysozyme. *Biochem. J.* **2016**, *473*, 3705–3724.

(51) Kast, K. M.; Brickmann, J.; Kast, S. M.; Berry, R. S. Binary Phases of Aliphatic N-Oxides and Water: Force Field Development and Molecular Dynamics Simulation. *J. Phys. Chem. A* **2003**, *107*, 5342–5351.

(52) Arakawa, T.; Timasheff, S. N. Preferential Interactions of Proteins with Solvent Components in Aqueous Amino Acid Solutions. *Arch. Biochem. Biophys.* **1983**, *224*, 169–177.

(53) Felitsky, D. J.; Cannon, J. G.; Capp, M. W.; Hong, J.; Wynsberghe, A. W. V.; Anderson, C. F.; Record, M. T. The Exclusion of Glycine Betaine from Anionic Biopolymer Surface: Why Glycine Betaine Is an Effective Osmoprotectant but Also a Compatible Solute. *Biochemistry* **2004**, *43*, 14732–14743.

(54) Courtenay, E. S.; Capp, M. W.; Anderson, C. F.; Record, M. T. J. Vapor Pressure Osmometry Studies of Osmolyte-Protein Interactions: Implications for the Action of Osmoprotectants in Vivo and for the Interpretation of "Osmotic Stress" Experiments in Vitro. *Biochemistry* **2000**, *39*, 4455–4471.

(55) Ganguly, P.; Shea, J.-E. Distinct and Nonadditive Effects of Urea and Guanidinium Chloride on Peptide Solvation. *J. Phys. Chem. Lett.* **2019**, *10*, 7406–7413.

(56) Adamczak, B.; Kogut, M.; Czub, J. Effect of Osmolytes on the Thermal Stability of Proteins: Replica Exchange Simulations of Trp-cage in Urea and Betaine Solutions. *Phys. Chem. Chem. Phys.* **2018**, *20*, 11174–11182.

(57) Schneider, C. P.; Trout, B. L. Investigation of Cosolute-Protein Preferential Interaction Coefficients: New Insight into the Mechanism by Which Arginine Inhibits Aggregation. *J. Phys. Chem. B* **2009**, *113*, 2050–2058.